

Current-induced Phase Transition in Ni Nanowires

N. Nurgazizov¹, A. Bukharaev^{1,2,*}, D. Biziaev¹, A. Chuklanov¹, T. Khanipov^{1,2}

¹ *Zavoisky Physical-Technical Institute, 10/7, Sibirsky tract, 420029 Kazan, Russia*

² *Kazan Federal University, 18, Kremlevskaya St., 420008 Kazan, Russia*

(Received 25 June 2012; published online 22 August 2012)

The single ferromagnetic Ni nanowires connecting two contact pads on the silicon oxide surface were fabricated using the scanning probe nanolithography technique based on the nanoindentation of polymethylmethacrylate resist and lift-off process. Wires with height from 9 to 26 nm, wide from 200 to 500 and length from 5 to 13 μm were obtained. The atomic and magnetic force microscopy was used to study the morphology and domain structure of the obtained nanowires. Multidomain and single-domain structures depending on the width of the nanowires were observed. Current-induced phase transition from ferromagnetic to paramagnetic state in the Ni nanowires was observed when studying of current-voltage characteristics of such nanostructures. This phenomenon is explained by the Joule heating of ferromagnetic Ni nanowires by the high-density current over Curie temperature.

Keywords: Scanning probe microscopy, Nanowires, Spin transfer torque.

PACS numbers: 68.37.Rt, 72.25.Ba

1. INTRODUCTION

Recently the high-density current flow through ferromagnetic nanowires (FNW) has been intensively studied [1-4]. When the high-density current ($\sim 10^{10}$ A/m²) flows through an FNW, a nonlinear change of the resistance is observed. This is due to the change of the internal structure of the FNW, occurring through the transfer of the electron spins to the crystal lattice. With the further increase in the current density Joule heating of FNW becomes significant and the nonlinear resistance behavior is related to the ferromagnet-paramagnetic state transition above Curie point [1,2]. The temperature variation of the magnetic nanostructures by the current of necessary magnitude is the basis of development of the new energy-independent devices with the super high density of data storage (thermally assisted MRAM). This type of recording and storage is based on the spin transition and has recently attracted much attention worldwide.

2. RESULTS AND DISCUSSION

Recently we experimentally observed the ferromagnetic-paramagnetic transition in nickel nanocontacts [5]. This work is devoted to the detection and study of this effect in Ni nanowires.

Single Ni FNWs that connect two contact pads on the silicon oxide surface were fabricated by the scanning probe nanolithography technique based on the polymer thin film nanoindentation of polymethylmethacrylate (PMMA) and lift-off process [6].

According to this method, after the formation of the polymer film with the windows of the desired size (lithography mask) a thin metal layer was deposited on the sample. The thickness of the metal layer should be less than that of the polymer film. The mask is chemically dissolved after the deposition. Thus only the metal deposited through the mask remains on the surface. Silicon oxide on the Si surface is necessary for studying

the current flow process through the FNW. The polymer resist layer on the sample surface was formed by coating a spinning sample with a chlorobenzene PMMA solution. A PMMA layer 30 – 40 nm thick was formed on the SiO₂ surface when chlorobenzene was dried. The thickness of the PMMA was determined on a scanning probe microscope (SPM) by the height of the step at the edge of the film. During the lithography process the PMMA thickness is controlled by the force curves, which reflect the interaction between the cantilever tip and the substrate. By analyzing characteristic inflections on the force curves one can determine the points of the tip contact with the PMMA surface and the solid SiO₂ substrate.

A lithography mask was drawn by the Solver P47 (NT-MDT) scanning probe microscope. The NSG20 (NT-MDT, force constant of 48 N/m) and NSC15 tips (MikroMasch, force constant of 46 N/m) with the tip apex curvature of about 10 nm were used. The NSC19 tips (MikroMasch, force constant 5 of N/m) with the CoCr coating were used for magnetic force measurements.

The single-step indentation was used for obtaining PMMA windows in the form of a continuous trench. The sequence of indentation points was specified in the way that they were rather close to each other. The experiments showed that the density of 50 points/ μm is sufficient to produce a trench with smooth edges. The minimum sufficient interaction time is 0.1 s at each point. To study the current flow through FNW, it was necessary to form contact pads. To this end, the windows $50 \times 50 \mu\text{m}$ were formed in the PMMA layer by the standard nano-engraving technique. Then they connected with a trench prepared by the single-step indentation.

The Ni thin film was deposited on the sample surface shaped by the mask in the Multiprobe P (Omicron) setup by the electron beam that evaporated the 99.9% Ni target in vacuum of $1 \cdot 10^{-6}$ Pa. The Solver P47 micro-

* a_bukharaev@kfti.knc.ru

scope working in AFM and MFM mode was used to study the morphology and domain structure of the FNW. Wires with the height of 9–26 nm, width of 200–500 nm and length of 5–20 μm were obtained.

In-plane magnetic domains were observed on these nanowires. The domains were directed along the wire axis for wire width of less than 400 nm and perpendicular to the wire axis for the wire width above 400 nm. A typical AFM image of the Ni nanowire (20 μm long, 240 nm wide and 13 nm high) is shown in Fig. 1a. The magnetic (phase) image of the same nanowire is shown in Fig. 1b. The magnetic image was obtained by the one-pass technique, when the magnetic tip moves at a large distance from the sample surface. The magnetization reversal of the nanowire was observed in the two-pass technique. This means that the obtained nanowire has low coercivity.

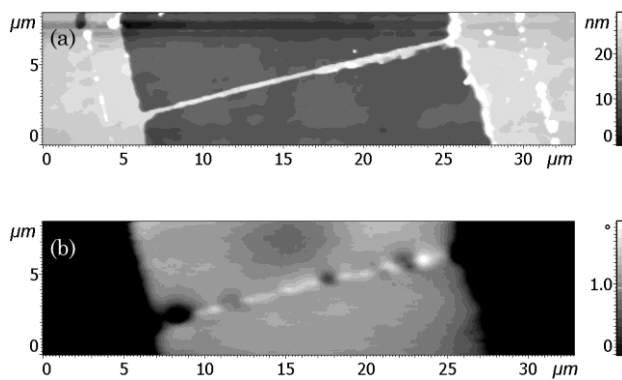


Fig. 1 – AFM and MFM images of FNW

Processes of the current flow through these FNWs were studied in low vacuum of 10^{-1} Pa in the chamber of the Solver HV (NT–MDT) microscope, in order to prevent the wire oxidation when heating to high temperatures. We improved this Solver HV microscope to carry out volt-ampere characteristic (VAC) measurements at the temperatures in the range from 25 to 200 $^{\circ}\text{C}$. VACs

REFERENCES

1. A. Yamaguchia, S. Nasu, H. Tanigawa, T. Ono, K. Miyake, K. Mibu, T. Shinjo, *Appl. Phys. Lett.* **86**, 012511 (2005).
2. A Yamaguchi, A Hirohata, T. Ono, H. Miyajima, *J. Phys.-Condens. Mat.* **24**, 024201 (2012).
3. M. Klaui, P.O. Jubert, R. Allenspach, A. Bischof, J.A.C. Bland, G. Faini, U. Rudiger, C.A.F. Vaz, L. Vila, C. Vouille, *Phys. Rev. Lett.* **95**, 026601 (2005).

were measured using a standard voltmeter-ammeter method by applying a saw-shape pulse with the frequency of 1 Hz and amplitude of up to 8 V to a sample. We could recalculate the resistance–current curves $R(I)$ into the resistivity–current density curves $\rho(j)$ on the basis on geometrical wire parameters. The finite-difference derivative of $\rho(j)$ curves makes it possible to find the point of the ferromagnetic–paramagnetic transition of FNW. This transition is observed as a sharp peak on the $d\rho(j)/dj$ curves when the current density reaches a critical value, at which FNW is heated above the Curie temperature by the current and the electron energy dispersion mechanism is changed. The increase in the initial temperature of FNW (by additional heating of the substrate) leads to the strong decrease in the critical current density value (Table 1) that is necessary for heating FNW up to the Curie temperature. This is a direct experimental proof that extremum point on the $d\rho(j)/dj$ curves is caused by the FNW phase transition from the ferromagnetic to the paramagnetic state.

Table 1 – Critical current and critical resistivity vs base temperature for Ni nanowire with 23 nm height, 310 nm wide, and 10.2 μm length

T, $^{\circ}\text{C}$	Critical current density (j), A/m^2	Critical resistivity (ρ), Ohm m
35	8.1	$3.63 \cdot 10^{-7}$
60	7.6	$3.86 \cdot 10^{-7}$
90	6.8	$4.00 \cdot 10^{-7}$
130	5.9	$4.15 \cdot 10^{-7}$
170	4.6	$4.24 \cdot 10^{-7}$
190	4	$4.27 \cdot 10^{-7}$

ACKNOWLEDGEMENTS

This work was supported partially by the grant of the Russian Foundation for Basic Research (Grant No. 12-02-00820) and by the programs of Russian Academy of Sciences.

4. G. Meier, M. Bolte, R. Eiselt, B. Kruger, D.-H. Kim, and P. Fischer, *Phys. Rev. Lett.* **98**, 187202 (2007).
5. R.G. Gatiyatov, V.N. Lisin, A.A. Bukharaev, *Appl. Phys. Lett.* **96**, 093108 (2010).
6. A.A. Bukharaev, D.A. Bizyaev, N.I. Nurgazizov, T.F. Khanipov, *Russian Microelectronics* **41** No2, 78 (2012).